Terminal Platinum(II) Perfluoroacyl Phosphido Complexes: Synthesis and Dynamic Processes

Denyce K. Wicht and David S. Glueck*

Department of Chemistry, Dartmouth College, 6128 Burke Laboratory, Hanover, New Hampshire 03755

Louise M. Liable-Sands and Arnold L. Rheingold

Department of Chemistry, University of Delaware, Newark, Delaware 19716

Received May 18, 1999

The Pt(II) phosphido methyl complexes Pt(dppe)(Me)(PPhR) (dppe = $Ph_2PCH_2CH_2PPh_2$, R = *i*-Bu, **1**; R = Is = 2,4,6-(*i*-Pr)$_3C_6H_2$, **2**) have been prepared by proton transfer from secondary phosphines to the methoxide ligand of Pt(dppe)(Me)(OMe). Oxidative addition of $ClC(O)C_3F_7$ to $Pt(PPh_2Me)_4$ gives *trans*-$Pt(PPh_2Me)_2(COC_3F_7)(Cl)$ (**3**); treatment of **3** with dppe yields Pt(dppe)(COC_3F_7)(Cl) (**4**). Complexes **3**·0.5CH_2Cl_2 and **4** were structurally characterized by X-ray crystallography. Reaction of **4** with $AgBF_4$ and a secondary phosphine or treatment of [Pt(dppe)(COC_3F_7)(NCMe)][BF_4] (**5**) with a secondary phosphine gives the cations [Pt(dppe)(COC_3F_7)(PHPhAr)][BF_4] (Ar = Mes = 2,4,6-$Me_3C_6H_2$, **6**; Ar = *o*-anisyl, **7**; Ar = Is, **8**; Ar = Mes-F_9 = 2,4,6-$(CF_3)_3C_6H_2$, **9**; Ar = Ph, **10**). Deprotonation of the cations with $LiN(SiMe_3)_2$ affords the phosphido complexes Pt(dppe)(COC_3F_7)(PPhAr) (Ar = Mes, **11**; Ar = *o*-anisyl, **12**; Ar = Is, **13**; Ar = Mes-F_9, **14**; Ar = Ph, **15**). Fluxional processes in complexes **11**−**15** were studied by variable-temperature multinuclear NMR spectroscopy; the spectra are consistent with rapid phosphorus inversion on the NMR time scale at room temperature.

Introduction

Pyramidal inversion at phosphorus in metal phosphido complexes is rapid on the NMR time scale.[1] This process has been studied in complexes containing two chiral centers; fast exchange gives an averaged NMR spectrum, and signals due to the two different diastereomers are observed when exchange is slow at low temperature.[1a,b,d,i] In the accompanying article, for example, we report NMR data characterizing rapid inversion at phosphorus in the chiral platinum(II) phosphido complexes Pt(diphos)(R)(PR′R″).[2] A disadvantage of this approach is that one diastereomer may be so much higher in energy than the other that it is not observed, so the barrier to the dynamic process cannot be measured experimentally. To avoid this problem, phosphorus inversion can be studied in complexes with one chiral center. If two diastereotopic nuclei are present, these exhibit different NMR chemical shifts if inversion is slow on the NMR time scale, and rapid inversion at phosphorus makes them equivalent. For example, Malisch obtained a phosphido inversion barrier of 14.4 kcal/mol in W(Cp)$(CO)_2(PMe_3)$(P(*i*-Pr)$_2$) by analysis of the dynamic ^{1}H NMR behavior of the isopropyl methyl groups.[1e] Here we report variable-temperature NMR studies of the complexes Pt(dppe)(R)(PPhR′), which contain diastereotopic nuclei either in a phosphido substituent or in a perfluoroacyl group coordinated to platinum.

Results and Discussion

The phosphido methyl complexes Pt(dppe)(Me)(PPh*i*-Bu) (**1**) and Pt(dppe)(Me)(PPhIs) (Is = 2,4,6-(*i*-Pr)$_3C_6H_2$, **2**), which contain diastereotopic *i*-Bu and *i*-Pr Me groups, respectively, were prepared by proton transfer from secondary phosphines to the methoxide ligand of Pt(dppe)(Me)(OMe).[3] The ^{1}H NMR spectrum (toluene-d_8) of previously reported[4] **1** at room temperature exhibits a doublet ($^3J_{HH}$ = 6 Hz, 6H) at δ 0.99, assigned to the *i*-Bu Me groups. This signal decreases in intensity and broadens to a single peak as the temperature is decreased to −15 °C. At −50 °C, two broad peaks begin to grow in, but they do not sharpen as the temperature is further decreased to −70 °C. These inconclusive

(1) For examples, see: (a) Zwick, B. D.; Dewey, M. A.; Knight, D. A.; Buhro, W. E.; Arif, A. M.; Gladysz, J. A. *Organometallics* **1992**, *11*, 2673−2685. (b) Buhro, W. E.; Zwick, B. D.; Georgiou, S.; Hutchinson, J. P.; Gladysz, J. A. *J. Am. Chem. Soc.* **1988**, *110*, 2427−2439. (c) Simpson, R. D.; Bergman, R. G. *Organometallics* **1992**, *11*, 3980−3993. (d) Crisp, G. T.; Salem, G.; Wild, S. B.; Stephan, F. S. *Organometallics* **1989**, *8*, 2360−2367. (e) Malisch, W.; Maisch, R.; Meyer, A.; Greissinger, D.; Gross, E.; Colquhoun, E. J.; McFarlane, W. *Phosphorus Sulfur* **1983**, *18*, 299−302. (f) Baker, R. T.; Whitney, J. G.; Wreford, S. S. *Organometallics* **1983**, *2*, 1049−1051. (g) Bonnet, G.; Kubicki, M. M.; Moise, C.; Lazzaroni, R.; Salvadori, P.; Vitulli, G. *Organometallics* **1992**, *11*, 964−967. (h) Fryzuk, M. D.; Joshi, K.; Chadha, R. K.; Rettig, S. J. *J. Am. Chem. Soc.* **1991**, *113*, 8724−8736. (i) Malisch, W.; Gunzelmann, N.; Thirase, K.; Neumayer, M. *J. Organomet. Chem.* **1998**, *571*, 215−222. (j) For a review, see: Rogers, J. R.; Wagner, T. P. S.; Marynick, D. S. *Inorg. Chem.* **1994**, *33*, 3104−3110.

(2) Wicht, D. K.; Kovacik, I.; Glueck, D. S.; Liable-Sands, L. M.; Incarvito, C. D.; Rheingold, A. L. *Organometallics* **1999**, *18*, 5141.

(3) Bryndza, H. E.; Calabrese, J. C.; Wreford, S. S. *Organometallics* **1984**, *3*, 1603−1604.

(4) Wicht, D. K.; Paisner, S. N.; Lew, B. M.; Glueck, D. S.; Yap, G. P. A.; Liable-Sands, L. M.; Rheingold, A. L.; Haar, C. M.; Nolan, S. P. *Organometallics* **1998**, *17*, 652−660.

10.1021/om9903691 CCC: $18.00
Publication on Web 11/22/1999

observations were further complicated by the overlap of this methyl signal with that of the Pt−Me group (m, δ 1.06−0.98).

The $^{13}C\{^1H\}$ NMR spectrum of phenyl(isobutyl)-phosphine shows two signals due to the diastereotopic Me carbons at δ 24.2 and 24.1 (C_6D_6); each exhibits $^3J_{PC}$ = 8 Hz. In contrast, in the $^{13}C\{^1H\}$ NMR spectrum of **1** (C_6D_6), the Me signal appears as a doublet ($^3J_{PC}$ = 7 Hz) at δ 25.2. This could be due either to rapid inversion at phosphorus or to the two diastereotopic Me groups having the same chemical shifts. Further study of **1** was hampered by its rapid decomposition in solution.

Diarylphosphido complex **2**, an orange-yellow solid, is stable in solution and has a ^{31}P NMR spectrum similar to those of previously reported Pt(dppe)(Me)-(PRR′) complexes.[4] In the ^1H NMR spectrum (toluene-d_8) at room temperature, the signal for the ortho *i*-Pr Me groups is a doublet ($^3J_{HH}$ = 7 Hz, 12H) at δ 1.21; the same chemical shift and coupling constant are observed for these protons in the ^1H NMR spectrum (C_6D_6) of the free phosphine PHPhIs.[5] This signal in **2** broadens as the temperature is lowered and begins to decoalesce into two peaks at −35 °C. However, at lower temperatures, all the ^1H NMR signals become broad and complete decoalescence is indiscernible.

In the $^{13}C\{^1H\}$ NMR spectrum (toluene-d_8), the *o*-*i*-Pr Me signal is a sharp singlet at δ 25.7. At −15 °C, the ^{31}P NMR signals for the dppe phosphorus trans to the methyl and for the phosphido ligand become broad and low in intensity. This broadening continues until −70 °C, when both signals completely disappear into the baseline.[6] However, at this temperature, the signal for the dppe phosphorus trans to the phosphido ligand remains sharp and neither the chemical shift nor the coupling constants change.

The NMR observations in **1** and **2** are consistent with rapid inversion at phosphorus, but could also be explained if the diastereotopic Me groups have coincident chemical shifts. Therefore, to exploit the larger chemical shift dispersion of ^{19}F NMR in comparison to ^1H NMR spectra, we prepared complexes containing diastereotopic CF_2 groups.

Bennett and co-workers previously reported oxidative addition of $ClC(O)CF_3$ and $ClC(O)C_2F_5$ to $Pt(PPh_2Me)_4$.[7] A similar reaction with the perfluoropropyl analogue gives *trans*-$Pt(PPh_2Me)_2(COC_3F_7)(Cl)$ (**3**). Addition of dppe to a solution of **3** gives the cis compound Pt(dppe)-$(COC_3F_7)(Cl)$ (**4**) (Scheme 1). ^{31}P and ^{19}F NMR data for **4** and its derivatives **5**−**15** (see below) are given in Tables 1 and 2.

The ^{31}P NMR spectrum of **3** ($CDCl_3$) shows a triplet at δ 6.5 ($^2J_{PF}$ = 5 Hz, $^1J_{Pt-P}$ = 2916 Hz). In the ^{19}F NMR spectrum ($CDCl_3$), the signal for the CF_3 group is a well-resolved triplet at δ −81.2 with F−F coupling of 9 Hz. Under some conditions, the CF_2 resonances in this and the subsequent compounds are multiplets (δ −111.5 to −111.6 ($COCF_2$) and δ −127.6 to −127.7 (CF_2CF_3) for **3**). However, we usually observed them as broad singlets. The C═O stretch observed in the IR (KBr) spectrum at 1672 cm^{-1} is similar to those reported for $Pt(PPh_2Me)_2(COCF_3)(Cl)$ (1670 cm^{-1}) and $Pt(PPh_2Me)_2$-$(COC_2F_5)(Cl)$ (1675 cm^{-1}).[7] IR data for the perfluoroacyl derivatives **4**−**15** (see below) are similar.

Scheme 1

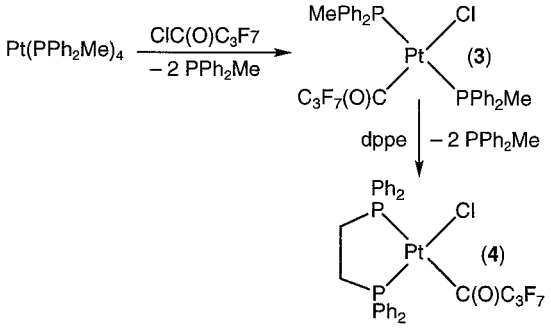

The X-ray crystal structures of **3**·$0.5CH_2Cl_2$ and **4** are shown in Figures 1 and 2, respectively; selected bond lengths and angles are given in the figure captions. The crystallographic data are given in Table 3, and further details are in the Experimental Section and the Supporting Information.

The crystal structure of **3** shows the expected square planar geometry at platinum; the angles around the metal center range from 89.70(6)° to 90.6(2)°. The structure is similar to that of the related complex *trans*-$Pt(PPh_2Me)_2(COCF_3)(Cl)$.[8] The Pt−Cl, Pt−C(O), and carbonyl bond lengths for **3** (2.402(2), 1.990(7), and 1.191(9) Å, respectively) are the same within experimental error as those in the trifluoroacyl complex (2.390(1), 2.028(6), and 1.210(5) Å). The Pt−P bond lengths are slightly longer in **3** (2.332(2) and 2.338(2) Å) than in the trifluoroacyl complex (2.316(1) and 2.321-(1) Å), although the difference is small.

The structure of **4** shows a slightly distorted square planar geometry due to the P−Pt−P bite angle of 85.71-(3)° imposed by the dppe ligand. The Pt−Cl bond in **4** (2.3774(10) Å) is slightly shorter than the Pt−Cl bond in **3** (2.402(2) Å), consistent with a larger trans influence for the perfluoroacyl ligand than for the phosphine. The Pt−C(O) and carbonyl bond lengths in **4** are 2.051(3) and 1.221(4) Å, respectively. The Pt−phosphine bond lengths are 2.3525(9) Å for the P trans to COC_3F_7 and 2.2431(9) Å for the P trans to Cl; these results and the $^1J_{Pt-P}$ values suggest that the perfluoroacyl ligand has a greater trans influence than Cl.

Treatment of **4** with $AgBF_4$ generates the acetonitrile cation $[Pt(dppe)(COC_3F_7)(NCMe)][BF_4]$ (**5**) (Scheme 2), whose ^{31}P NMR spectrum is similar to that of the previously reported methyl complex [Pt(dppe)(Me)(NC-Me)][BF_4].[9] The cationic complexes $[Pt(dppe)(COC_3F_7)$-$(PHPhAr)][BF_4]$ (Ar = Mes = 2,4,6-$(Me)_3C_6H_2$, **6**; Ar = *o*-anisyl, **7**; Ar = Is, **8**; Ar = Mes-F_9 = 2,4,6-$(CF_3)_3C_6H_2$, **9**; Ar = Ph, **10**) were prepared by treatment of **5** with the appropriate phosphine or directly from **4** (Scheme 2). The ^{31}P NMR spectra of **6**−**10** (Table 1) exhibit the expected AMX patterns with the resonances due to the coordinated phosphines appearing upfield between δ −7

(5) Brauer, D. J.; Bitterer, F.; Dörrenbach, F.; Hebler, G.; Stelzer, O.; Krüger, C.; Lutz, F. *Z. Naturforsch.* **1996**, *51B*, 1183−1196.

(6) The accompanying article (ref 2) reports similar observations for Pt(*S*,*S*-Chiraphos)(Me)(PPhIs). We assume that the unusual broadness observed in the ^{31}P NMR spectrum is due to a dynamic process involving rotation around the Pt−PPhIs bond (see below).

(7) Bennett, M. A.; Chee, H.-K.; Robertson, G. B. *Inorg. Chem.* **1979**, *18*, 1061−1070.

(8) Bennett, M. A.; Ho, K.-C.; Jeffery, J. C.; McLaughlin, G. M.; Robertson, G. B. *Aust. J. Chem.* **1982**, *35*, 1311−1321.

(9) In $CDCl_3$, δ 49.1 ($^1J_{Pt-P}$ = 1809 Hz, P trans to Me) and δ 38.9 ($^1J_{Pt-P}$ = 4370, P trans to NCMe). Appleton, T. G.; Bennett, M. A. *Inorg. Chem.* **1978**, *17*, 738−747.

Table 1. ^{31}P NMR Data for [Pt(dppe)(COC_3F_7)(X)]$^{n+}$ Complexes[a−d]

X	no.	$\delta(P_1)$ (J_{Pt-P})	$\delta(P_2)$ (J_{Pt-P})	$\delta(P_3)$ (J_{Pt-P})	J_{12}	J_{13}	J_{23}
Cl	**4**	34.8 (3931)	36.4 (1755)		8		
NCMe	**5**	30.6 (4087)	42.1 (1755)		8		
PH(Ph)(Mes)	**6**	46.6 (2695)	42.3 (1688)	−33.0 (2524)	9	306	24
PH(Ph)(*o*-An)	**7**	47.5 (2207)	44.2 (1627)	−21.3 (2672)	10	314	24
PH(Ph)(Is)	**8**	40.7 (2682)	40.0 (1634)	−31.5 (2554)	9	305	23
PH(Ph)(Mes-F_9)	**9**	44.3 (2942)	41.8 (1622)	−12.2 (2724)	10	325	21
$PHPh_2$	**10**	48.2 (2713)	44.7 (1631)	−7.9 (2576)	9	304	22
P(Ph)Mes)	**11**	46.3 (1869)	39.9 (1865)	−14.0 (949)	8	107	5
P(Ph)(*o*-An)	**12**	47.2 (1898)	42.3 (1782)	−28 (v. broad)	9	86	
(−50 °C)	**12a**	49.3 (1950)	43.5 (1759)	−22.4 (1103)		99	
(1.3:1 ratio)[e]	**12b**	47.5 (1877)	45.6 (1798)	−39.6 (880)		82	
P(Ph)(Is)	**13**	41.0 (1865)	31.6 (1836)	−28.4 (989)		106	
(−70 °C)	**13a**	46.8 (1920)	30.5 (1830)	−27.2 (1060)		112	
(1.7:1 ratio)[a]	**13b**	39.9 (broad)	38.7 (broad)	−25.6 (broad)		102	
P(Ph)(Mes-F_9)	**14**	39.5 (2100)	33.5 (1743)	4.0 (1096)		111	
(−70 °C)		39.4 (2096)	29.7 (1717)	−6.5 (1060)		111	
PPh_2	**15**	45.7 (1880)	42.3 (1816)	−1.6 (894)	11	92	12

[a] $n = 0$ for **4** and **11**−**15**; $n = 1$ for **5**−**10**. [b]Temperature = 22 °C except where noted. Chemical shifts in ppm, external reference 85% H_3PO_4, coupling constants in Hz. [c]P_1 and P_2 are the dppe P nuclei; P_3 is trans to P_1. [d]Solvents: CD_2Cl_2 for **4**, **6**, **7**, **9**, **10**; $CDCl_3$ for **5**, **8**; THF-d_8 for **11**, **12**, **15**; toluene-d_8 for **13**, **14**. [e]Labels: major isomer **a**, minor isomer **b**.

Table 2. ^{19}F NMR Data for [Pt(dppe)(COC_3F_7)(X)]$^{n+}$ Complexes[a,b,c]

X	no.	$\delta(CF_3)$[d]	$\delta(COCF_2)$ (J_{FF})	$\delta(CF_2CF_3)$ (J_{FF})
Cl	**4**	−81.6	−112.9 to −113.0 (m)	−126.5 to −126.6 (m)
NCMe	**5**	−81.2	−114.4	−127.0
PH(Ph)(Mes)	**6**	−81.6	−112.6	−127.4
PH(Ph)(*o*-An)	**7**	−81.7	−112.6, −114.2 (314)	−127.5 to −127.6 (m)
PH(Ph)(Is)	**8**	−81.5	−111.5, −112.5 (307)	−126.6, −127.5 (300)
PH(Ph)(Mes-F_9)[e]	**9**	−79.1	−109.8 (broad)	−124.5
$PHPh_2$	**10**	−81.6	−113.2	−127.3
P(Ph)(Mes) (70 °C)	**11**	−82.6	−112.9	−127.7
(−15 °C)		−82.6	−111.5, −114.4 (308)	−127.7
P(Ph)(*o*-An) (60 °C)	**12**	−82.0	−113.2	−127.1
(−50 °C)	**12a**	−82.0[f]	−114.9, −117.1 (306)	−128.6, −129.9 (310)
(1.3:1 ratio)	**12b**		−114.0, −115.3 (313)	−129.4
P(Ph)(Is) (60 °C)	**13**	−81.2	−112.2	−126.7
(−70 °C)	**13a**	−81.2[f]	−112.4, −115.3 (310)	−127.4 (broad)
(1.7:1 ratio)	**13b**		−111.6 to −112.1 (m)	−127.1 (broad)
P(Ph)(Mes-F_9) (60 °C)	**14**	−81.3	−111.8	−126.8
(−70 °C)	**14a**	−81.6	−111.7 (broad m)	−127.0, −128.6 (300)
(5:1 ratio)	**14b**	−81.1		
PPh_2	**15**	−81.4	−112.2	−126.7
(−40 °C)		−81.4	−112.9, −113.9 (308)	−127.9, −128.9 (308)

[a] $n = 0$ for **4** and **11**−**15**; $n = 1$ for **5**-**10**. For cations **5**−**10**, an additional peak due to the BF_4 anion was observed near −153 ppm. [b] Temperature = 22 °C except where noted. Chemical shifts in ppm, external reference $CFCl_3$, coupling constants in Hz. [c] Solvents: CD_2Cl_2 for **4**, **6**, **7**, **9**, **10**; $CDCl_3$ for **5**, **8**, THF-d_8 for **11**, **12**, **15**; toluene-d_8 for **13**, **14**. [d] The CF_3 signals are triplets with J_{FF} values of 9−10 Hz. [e] Additional data for Mes-F_9 derivatives: for **9** δ −53.2 (d, $^4J_{FP} = 12$, *o*-CF_3), −61.8 (*p*-CF_3); for **14** δ −55.5 (d, $^4J_{PF} = 42$, *o*-CF_3), −63.6 (*p*-CF_3). For **14** at −70 °C, see text, and δ −56.8 (broad), −63.2 and −62.9 (5:1 ratio, *p*-CF_3). [f] Different CF_3 resonances were not observed for the two isomers.

and −33. The large $^2J_{PP(trans)}$ (304−325 Hz), $^1J_{Pt-P}$ (2500−2700 Hz), and $^1J_{PH}$ (388−410 Hz) are characteristic of cationic Pt(II) phosphine complexes.[9] The signal for the coordinated phosphine PHPhMes-F_9 in **9** is quite broad, presumably due to P−F coupling.

The presence of a chiral phosphorus center in **6**−**9** makes the fluorine atoms of the CF_2 groups diastereotopic. However, due to accidental chemical shift equivalence in **6** and **9**, the perfluoroacyl ligands in these complexes show only three signals, with chemical shifts and F−F coupling constants similar to those for **3**−**5** (Table 2). As expected, a similar ^{19}F NMR spectrum is observed for **10**, because the phosphido ligand is symmetric. In the case of **7** and **8**, however, the CF_2 fluorine signals are AB patterns that exhibit F−F coupling. In **8**, the ortho *i*-Pr Me groups are diastereotopic; two signals appear at δ 0.95 (d, $^3J_{HH} = 7$ Hz, 6H) and 0.76 (broad, 6H).

Deprotonation of the cationic complexes **6**−**10** with $LiN(SiMe_3)_2$ affords the neutral Pt(II) phosphido complexes Pt(dppe)(COC_3F_7)(PPhAr) (Ar = Mes, **11**; Ar = *o*-anisyl, **12**; Ar = Is, **13**; Ar = Mes-F_9, **14**; Ar = Ph, **15**) (Scheme 2). These yellow or orange solids were characterized by NMR (^{1}H, ^{31}P, ^{19}F) spectroscopy, IR spectroscopy, and elemental analysis. They are stable in the solid state, but decompose slowly in solution to unidentified products. The phosphido resonances are observed in the ^{31}P NMR spectra from δ 4.0 to −28.4 (Table 1). The signal due to the phosphido ligand in **14** is very broad, presumably as a consequence of P−F coupling to the ortho CF_3 groups of Mes-F_9. As expected, the observed P−P(trans) couplings (∼90−120 Hz) and Pt−P couplings (∼900−1100 Hz) are small in comparison to those of the coordinated phosphine precursors **6**−**10**, because of decreased s-character in the Pt−phosphido bond upon deprotonation.[10]

Variable-Temperature NMR Behavior. As in the cationic precursors, the chiral phosphorus centers in **11**−**14** make the fluorines in the CF_2 groups diastereotopic, as observed in variable-temperature ^{19}F NMR

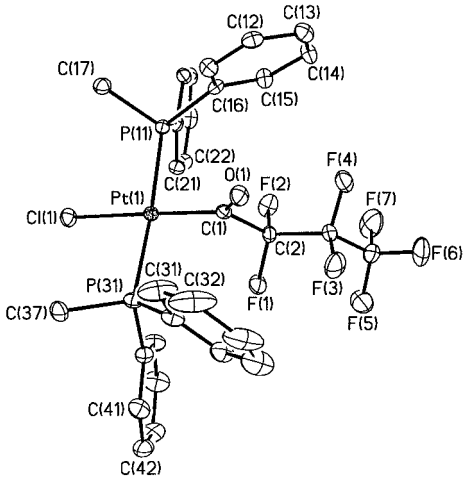

Figure 1. ORTEP diagram of **3**·0.5CH_2Cl_2 with thermal ellipsoids at 30% probability. Solvent molecule and hydrogen atoms are omitted for clarity. Selected bond lengths (Å) and angles (deg): Pt−C(1) = 1.990(7), Pt−Cl(1) = 2.402(2), Pt−P(31) = 2.338(2), Pt−P(11) = 2.332(2), C(1)−O(1) = 1.191(1), C(1)−Pt−P(11) = 90.6(2), P(11)−Pt−Cl(1) = 89.7(6), Cl(1)−Pt−P(31) = 89.95(7), P(31)−Pt−C(1) = 90.0(2), P(11)−Pt−P(31) = 173.23(5), C(1)−Pt−Cl(1) = 177.6(2).

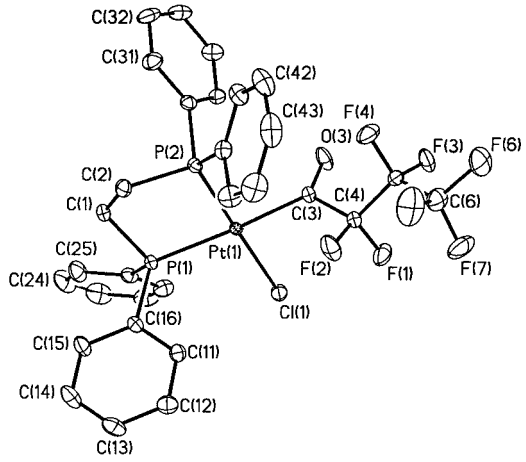

Figure 2. ORTEP diagram of **4** with thermal ellipsoids at 30% probability and hydrogen atoms omitted for clarity. Selected bond lengths (Å) and angles (deg): Pt−C(3) = 2.051(3), Pt−Cl(1) = 2.3774(10), Pt−P(1) = 2.3525(9), Pt−P(2) = 2.2431(9), C(3)−O(3) = 1.221(4), C(3)−Pt−P(2) = 92.32(10), P(2)−Pt−P(1) = 85.71(3), P(1)−Pt−C(1) = 96.18(3), Cl(1)−Pt−C(3) = 85.89(1), C(3)−Pt−P(1) = 176.72(10), P(2)−Pt−Cl(1) = 177.10(3).

spectra (Table 2). In some cases, variable-temperature ^{31}P and ^{1}H NMR spectra provided additional information about the dynamics of these molecules in solution.

For example, the ^{19}F NMR spectrum (THF-d_8) of Pt(dppe)(COC_3F_7)(PPhMes) (**11**) at 60 °C contains sharp signals due to the CF_3 and CF_2CF_3 groups, but a broad $COCF_2$ resonance. At room temperature this signal decoalesces into two peaks, and at −15 °C it is an AB quartet ($^2J_{FF}$ = 308 Hz) which continues to sharpen as the temperature is lowered to −50 °C. Some additional signal broadening was observed at −70 °C. The ^{31}P NMR peaks for **11** remain sharp from 60 to −15 °C; they broaden slightly at −35 °C and continue to decrease in intensity as the temperature reaches −70 °C. In the ^{1}H NMR spectra (THF-d_8), the sharp singlet observed for the two aryl *o*-Me groups at δ 2.44 (22 °C, 6H) does not broaden into the baseline until −70 °C, an indication that rotation around the P−C(Mes) bond does not appear to be restricted at lower temperatures.

Similar ^{19}F NMR decoalescence behavior resulting in AB quartets was observed at −50 °C for Pt(dppe)(COC_3F_7)(PPh*o*-anisyl) (**12**); in addition, two different isomers (1:1.3 ratio) were observed at this temperature by ^{19}F and ^{31}P NMR (Tables 1 and 2 and Figure 3). Variable-temperature ^{1}H NMR spectra are consistent with the ^{19}F and ^{31}P NMR results. At room temperature in the $^{1}H\{^{31}P\}$ NMR spectrum (THF-d_8), the OMe signal is a singlet at δ 3.85; at −50 °C the peak decoalesces into two peaks at δ 4.01 and 3.82 in a 1.3:1 ratio.

The variable-temperature NMR spectra of Pt(dppe)(COC_3F_7)(PPhIs) (**13**) are similar to those of **12**; at low temperature there is a 1.7:1 ratio of isomers (Tables 1 and 2). This behavior is also observed in the $^{1}H\{^{31}P\}$

Table 3. Crystallographic Data for *trans*-Pt(PPh_2Me)$_2$(COC_3F_7)(Cl) (3)·0.5CH_2Cl_2 and Pt(dppe)(COC_3F_7)(Cl) (4)

	3·0.5CH_2Cl_2	**4**
formula	$C_{30.5}H_{27}Cl_2F_7OP_2Pt$	$C_{30}H_{24}ClF_7OP_2Pt$
fw	870.45	825.97
space group	$P\bar{1}$	$P2_1/n$
a, Å	10.1465(2)	9.2231(2)
b, Å	12.2675(2)	27.2944(4)
c, Å	15.0834(3)	12.4868(3)
α, deg	102.9967(6)	90
β, deg	100.4318(9)	104.8681(8)
γ, deg	114.3832(6)	90
V, Å^3	1584.85(3)	3038.18(3)
Z	2	4
cryst color, habit	colorless rod	pale yellow rod
D(calc), g cm^{-3}	1.824	1.806
μ(Mo Kα), cm^{-1}	47.62	48.78
temp, K	223(2)	198(2)
diffractometer	Siemens P4/CCD	
radiation	Mo Kα (*λ* = 0.71073 Å)	
$R(F)$, %[a]	4.27	2.80
$R(wF^2)$, %[a]	14.49	5.87

[a] Quantity minimized = $R(wF^2) = \sum[w(F_o^2 - F_c^2)^2/\sum[(wF_o^2)^2]^{1/2}$; $R = \sum\Delta/\sum(F_o)$, $\Delta = |(F_o - F_c)|$

Scheme 2

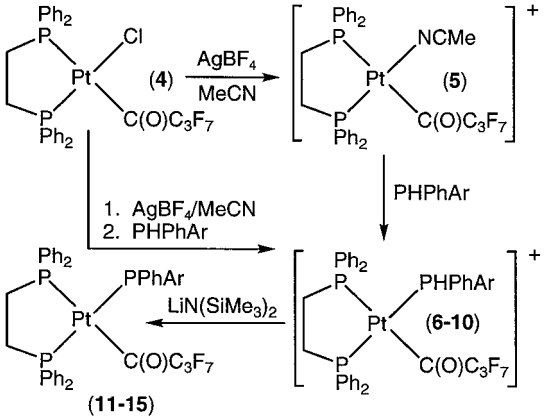

Ar = Mes (**6**, **11**); *o*-anisyl (**7**, **12**); Is (**8**, **13**); Mes-F_9 (**9**, **14**); Ph (**10**, **15**)

(10) (a) Bohle, D. S.; Jones, T. C.; Rickard, C. E. F.; Roper, W. R. *Organometallics* **1986**, *5*, 1612−1619. (b) Deeming, A. J.; Doherty, S.; Marshall, J. E.; Powell, J. L.; Senior, A. M. *J. Chem. Soc., Dalton Trans.* **1993**, 1093−1100. (c) Handler, A.; Peringer, P.; Müller, E. P. *J. Chem. Soc., Dalton Trans.* **1990**, 3725−3727. (d) Ref 1b.

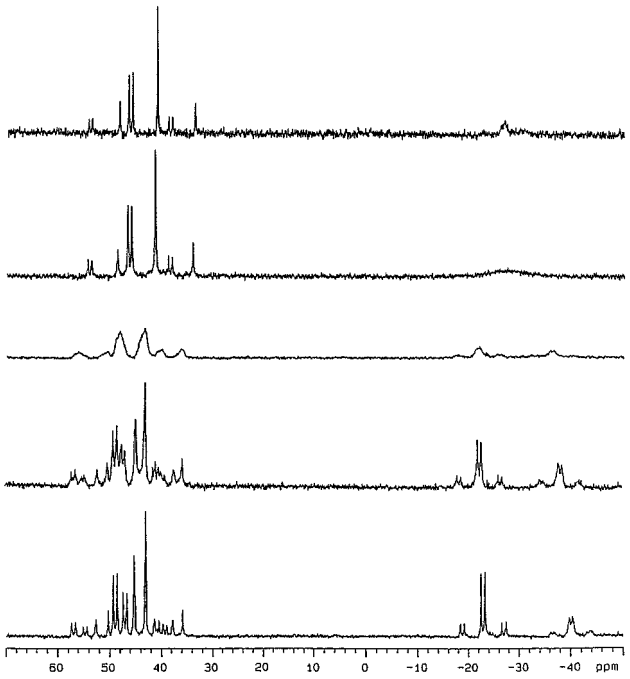

Figure 3. Variable-temperature $^{31}P\{^1H\}$ NMR spectra (THF-d_8) of Pt(dppe)(COC_3F_7)(PPh*o*-anisyl) (**12**) at the following temperatures: 60 °C (top), 22 °C, −15 °C, −34 °C, −50 °C (bottom).

NMR spectra of **13** (toluene-d_8). As in complex **2**, the ortho *i*-Pr Me groups give rise to a broad doublet at δ 1.19 (12H, $^3J_{HH}$ = 6 Hz) and a methine signal (m, δ 4.72−4.67). Both of these signals as well as the dppe CH_2 and aryl proton peaks broaden as the temperature is lowered. At −50 °C two new methine peaks begin to grow in, and at −70 °C the signals are broad and in a ratio of approximately 1.7:1 (δ 5.03 and 4.69).

The variable-temperature NMR data for the PPhMes-F_9 analogue (**14**) is somewhat more complicated because of the presence of the bulky Mes-F_9 group. At −15 °C, the signal for its equivalent ortho CF_3 groups decoalesces into two peaks at δ −54.8 and −56.2, presumably due to restricted rotation around the P−C(Mes-F_9) bond, and the two CF_2 resonances also broaden and split into two peaks at δ −111.6 and −112.0 ($COCF_2$) and δ −127.0 and −127.2 (CF_2CF_3). The ^{19}F NMR spectrum at −70 °C is complicated (Table 2). One of the two peaks due to the ortho CF_3 group splits; it is unclear if these are two different peaks at δ −54.1 and −54.4 or simply P−F coupling of 77 Hz. The other peak due to the ortho CF_3 group is slightly broad. Decoalesence into two peaks of different intensities (ca. 1:5) is also seen for the para CF_3 signal and the CF_2CF_3 group. The α CF_2 signal is a broad multiplet, and the β CF_2 resonance is an apparent AB quartet. The low-temperature ^{31}P NMR spectra, however, do not differ much from those at room temperature (Table 1), and ^1H NMR spectra were not particularly informative.

As shown in Figure 4, the low-temperature ^{19}F NMR spectra of the higher-symmetry complex Pt(dppe)-(COC_3F_7)(PPh_2) (**15**) are similar to those observed for **11**−**14**, with AB quartet signals observed for both CF_2 groups at −40 °C. The ^{31}P spectrum does not change at this temperature. The dppe CH_2 protons appear as two multiplets at δ 2.32−2.30 and δ 2.18−2.13 in the $^1H\{^{31}P\}$ NMR spectrum (THF-d_8) at room temperature.

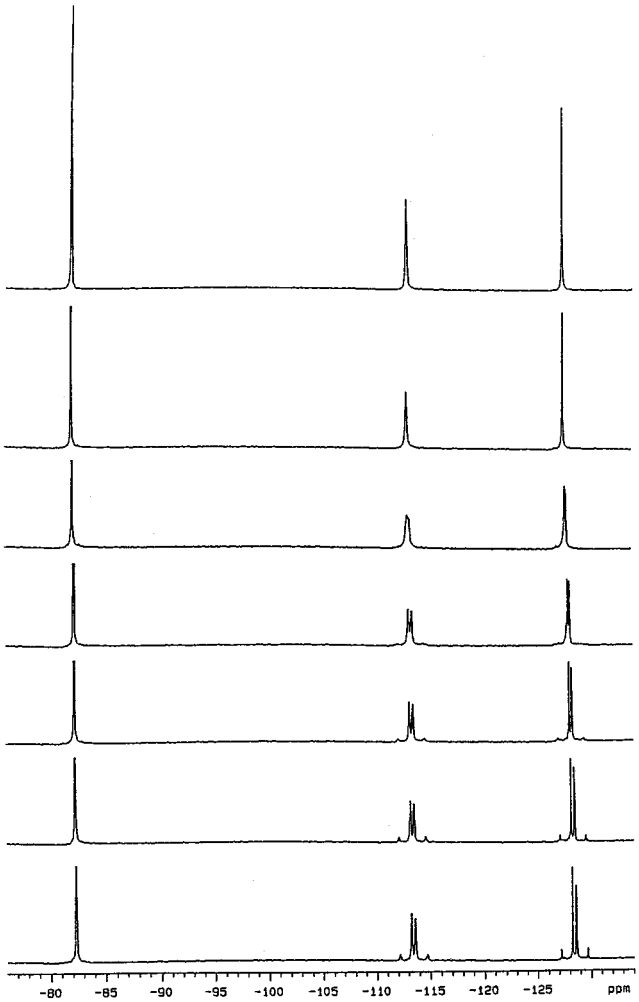

Figure 4. Variable-temperature ^{19}F NMR spectra (THF-d_8) of Pt(dppe)(COC_3F_7)(PPh_2) (**15**) at the following temperatures: 25 °C (top), 12 °C, −5 °C, −25 °C, −40 °C, −60 °C, −70 °C (bottom).

These peaks start to broaden at −5 °C and coalesce into one broad peak at −22 °C. The broad peak becomes sharper at lower temperatures; at −60 °C there are three signals at δ 2.64−2.60 (1H), 2.40−2.36 (1H), and 2.08−2.04 (2H) in the $^1H\{^{31}P\}$ NMR spectrum.

Measurement of the coalescence temperatures in the multinuclear NMR spectra of these complexes provides approximate free energies of activation for the dynamic processes.[11] The results are shown in Table 4. There is good agreement between data obtained from spectra of different nuclei, and the barriers (ca. 11−13 kcal/mol) are similar in this series of perfluoroacyl complexes.

Dynamic Processes. The perfluoroacyl groups in phosphido complexes **11**−**14** were intended to serve as ^{19}F NMR spectroscopic probes of phosphorus inversion. As described briefly in the Introduction, the diastereotopic fluorine nuclei in a CF_2 group are expected to have different NMR chemical shifts if inversion is slow on the NMR time scale, while rapid phosphorus inversion through a planar transition state makes them equivalent. As foreseen, the ^{19}F NMR signals due to the CF_2 groups in these compounds are singlets in the high-

(11) Friebolin, H. In *Basic One- and Two-Dimensional NMR Spectroscopy*, 2nd ed.; VCH: New York, 1993; pp 287−314. See the Experimental Section for more details and error analysis.

Table 4. Variable-Temperature NMR Data for Perfluoroacyl Pt(II) Phosphido Complexes[a]

complex	resonance[b]	$\Delta\nu$ (Hz)[c]	J_{AB} (Hz)[d]	T_c (K)	$\Delta G_c^{\ddagger}$ (kcal/mol)
11	$COCF_2$	818	308	295	12.7
12	$COCF_2$ (a)	367	313	253	10.9
	$COCF_2$ (b)	621	306	253	10.9
	CF_2CF_3	367	310	263	11.4
	*P*Ph(*o*-An)	2089		283	11.8
	cis dppe *P*	219		243	11.1
	trans dppe *P*	255		243	11.1
	O*Me*	57		243	11.8
13	$COCF_2$	818	310	278	11.9
15	$COCF_2$	282	308	263	11.4
	CF_2CF_3	282	308	263	11.4

[a] Solvent: THF-d_8 for **11**, **12** and **15**, toluene-d_8 for **13**. Estimated errors are different for each resonance; the largest estimated errors are on the order of 5 Hz in $\Delta\nu$ and J_{AB}, 10 °C in T_c, and 0.5 kcal/mol in $\Delta G_c^{\ddagger}$. Cis and trans are defined with respect to the phosphido ligand. [b]The italics indicate ^{19}F, ^{31}P, or ^{1}H nuclei. [c]$\Delta\nu$ values from slow-exchange spectra at 248 K (**11**), 223 K (**12**), 203 K (**13** and **15**). [d]J_{FF} in CF_2 from slow-exchange ^{19}F NMR spectra.

temperature limit, consistent with rapid inversion at phosphorus. In the low-temperature spectra, AB quartets are observed for the fluorine signals, consistent with slow inversion on the NMR time scale. The barriers calculated for these dynamic processes, ca. 11−13 kcal/mol, are similar to those reported for phosphorus inversion in other transition metal phosphido complexes.[1]

However, the observation of singlet resonances in the high-temperature ^{19}F NMR spectra might be due to accidental chemical shift equivalence of the diastereotopic CF_2 fluorine nuclei, as observed in the ^{19}F NMR spectra of two of the four cations (**6** and **9**). In this case, the low-temperature observations of inequivalent fluorines must be explained not by slow inversion, but by a different fluxional process.

Several dynamic processes could give rise to the observed ^{19}F NMR AB patterns. It is convenient to discuss each in terms of the highest symmetry conformation possible in these perfluoroacyl phosphido complexes, in which a plane of symmetry lies in the square plane of the molecule. The diastereotopic fluorines in a CF_2 group are equivalent in the high-symmetry conformation when the carbonyl group is in the square plane and the fluorine nuclei of each CF_2 group are positioned above and below the plane. This perfluoroacyl geometry should be accessible on the NMR time scale unless there is restricted rotation about the Pt−C or C−C bond, which seems unlikely, given the ca. 4 kcal/mol rotational barrier in C_2F_6.[12]

Slow interconversion between the two isomers (δ and λ) that are possible due to different dppe ring conformations (Chart 1) could remove the effective (square) plane of symmetry and make the fluorines of a CF_2 group inequivalent. However, literature reports suggest that the barrier to this process is lower than the ones we observe. Thus, $\delta-\lambda$ interconversion in the ruthenium complexes $[Ru(Cp)(dppe)(SR_2)]^+$ (R = Ph, Et; Chart 1, **A**) was found to have a barrier less than ca. 7 kcal/mol.[13]

Chart 1

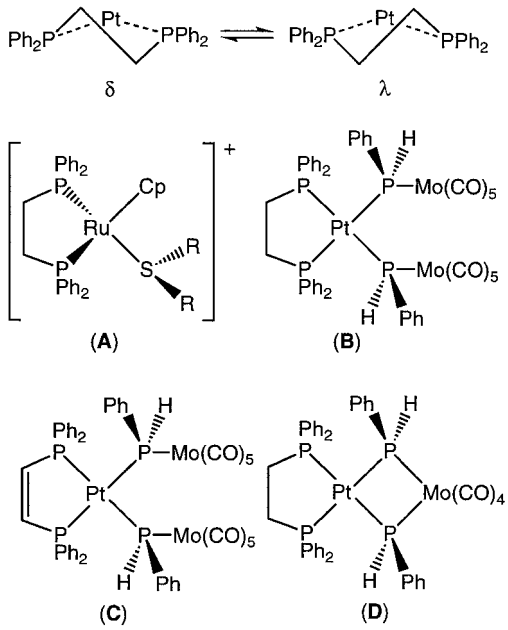

Similarly, Deeming and Doherty rejected $\delta-\lambda$ interconversion as a possible dynamic process to account for the low-temperature ^{31}P NMR observations in *meso*-Pt(dppe)(μ-PPhH)$_2${Mo(CO)$_5$}$_2$ (**B**, Chart 1).[14] For example, the analogous complex Pt($Ph_2PCH{=}CHPPh_2$)(μ-PPhH)$_2${Mo(CO)$_5$}$_2$ (**C**, Chart 1) exhibited similar fluxional behavior, although $\delta-\lambda$ interconversion is impossible with this rigid ligand. Consistent with these precedents, no evidence of dynamic behavior was found in the low-temperature ^{19}F NMR spectrum of Pt(dppe)(COC_3F_7)(Cl) (**4**).

The ^{31}P NMR observations on **B** and **C** were ascribed to restricted rotation around the Pt−μ-P bond. This conclusion was supported by the lack of dynamic behavior observed in Pt(dppe)(μ-PPhH)$_2${Mo(CO)$_4$} (**D**, Chart 1), where the single Mo center bridges the two phosphido ligands, thereby restricting rotation around the Pt−μ-P bonds. Hindered rotations similar to those observed in **B** and **C** have been observed in related complexes containing M-μ-PR_2 ligands.[15]

Similar slow rotation about Pt−P bonds may be occurring at low temperature in phosphido complexes **11**−**15**. In the perfluoroacyl complex with the highest symmetry, diphenylphosphido compound **15**, the fluorine nuclei of a CF_2 group can become equivalent at high temperature by rotation about the Pt−P bond; the phosphorus phenyl groups become equivalent when the P lone pair is in the square plane. Phosphorus inversion can also make the fluorines equivalent via the transition state in which the PC_2 unit is either coplanar with or perpendicular to the Pt square plane. Note that this requires Pt−P rotation to be unhindered so that the planar phosphido group can occupy the square plane of symmetry. The low-temperature ^{19}F NMR results for

(12) Gallaher, K. L.; Yokozeki, A.; Bauer, S. H. *J. Phys. Chem.* **1974**, *78*, 2389−2395.
(13) Ohkita, K.; Kurosawa, H.; Hirao, T.; Ikeda, I. *J. Organomet. Chem.* **1994**, *470*, 179−182.
(14) Deeming, A. J.; Doherty, S. *Polyhedron* **1996**, *15*, 1175−1190.
(15) (a) Deeming, A. J.; Cockerton, B. R.; Doherty, S. *Polyhedron* **1997**, *16*, 1945−1956. (b) Dobbie, R. C.; Mason, P. R. *J. Chem. Soc., Dalton Trans.* **1976**, 189−191. (c) Maassarani, F.; Davidson, M. F.; Wehman-Ooyevaar, I. C. M.; Grove, D. M.; van Koten, M. A.; Smeets, W. J. J.; Spek, A. L.; van Koten, G. *Inorg. Chim. Acta* **1995**, *235*, 327−338.

15 thus require that *both* Pt−P rotation and P inversion be slow on the NMR time scale at low temperature.[16]

Since the aryl groups in unsymmetrical phosphido complexes **11**−**14** are bulkier than phenyl, it is likely that Pt−P(Ph)(Ar) rotation is also slow on the NMR time scale at low temperature for those compounds.[17] In these cases, inversion at phosphorus can make the fluorines of a CF_2 group equivalent only if the planar PC_2 unit of the phosphido group can occupy the square plane of the molecule. Thus, if restricted rotation about the Pt−P bond makes this impossible, rapid inversion may still occur, but the fluorine nuclei of a CF_2 group are inequivalent. In other words, unlike the situation for symmetrical PPh_2 complex **15**, Pt−P rotation alone cannot make the fluorines of a CF_2 group equivalent in **11**−**14**; P inversion is required to do this. Therefore, the observation in these cases of CF_2 singlet resonances in the ^{19}F NMR spectra at room temperature or above requires that P inversion is rapid on the NMR time scale at these temperatures. By extension, this process is also likely to be rapid for **15** at room temperature, although we cannot reach this conclusion from the data for **15** in isolation (that is, P inversion could have a high barrier for **15**, as long as Pt−P rotation was rapid at room temperature).

With these ideas in mind, it is possible to rationalize the observed low-temperature spectra of complexes **11**−**14**. For (*o*-anisyl)phenylphosphido complex **12**, the simplest explanation (A) for the observation of inequivalent fluorines (^{19}F NMR) and of two different isomers is that both phosphorus inversion and Pt−P rotation are slow on the NMR time scale at low temperature. In this case, the two observed isomers are diastereomers in which either the P−Ph or the P−anisyl group is close in space to the perfluoroacyl ligand. These isomers would be interconverted by a combination of Pt−P rotation and P inversion. The lack of symmetry of the anisyl group means that other combinations of dynamic processes could explain the spectroscopic observations. First, slow inversion at phosphorus plus slow rotation about the P−C(anisyl) bond (B) would give two diastereomers that differ in the position of the anisyl group. Second, slow Pt−P rotation plus slow P−C rotation (C) could give two analogous isomers, with the proviso (see above) that the PC_2 unit is not in the square plane. Due to its simplicity and in analogy with **13** and **14** (see below), we favor explanation A above.

If both P inversion and Pt−P rotation are slow in **11**, **13**, and **14**, we would also expect to see two different isomers. Therefore, the data for mesitylphosphido complex **11**, in which only one isomer is observed, are puzzling. They could be explained if one of the expected diastereomers were much higher in energy than the other, so it is not observed, i.e., if the Mes group is preferentially oriented close to the perfluoroacyl group. Alternatively, slow Pt−P rotation, which prevents the PPh(Mes) group from entering the square plane, would make the CF_2 fluorines inequivalent even if inversion were fast on the NMR time scale, as discussed for **15**.

For isityl- and fluoromesitylphosphido complexes **13** and **14**, the low-temperature NMR spectra are not as well-resolved as for **11**, **12**, and **15**. However, in both these cases, there is evidence for the existence of two low-temperature diastereomers, as is clear for anisyl complex **12**. As in that case, the simplest explanation of these observations is that both P inversion and Pt−P rotation are slow at low temperature. Although the ^{19}F NMR spectrum at −15 °C shows that rotation about the P−C(Mes-F_9) bond in **14** is slow, the symmetry of the Mes-F_9 group means that this process cannot give rise to the two isomers seen at this temperature. With these extremely bulky aryl groups, we cannot, however, rule out other conformational equilibria which might also lead to the inequivalence of the CF_2 fluorines.

According to these analyses, the dynamic processes for which barriers were extracted from the NMR spectra involve a *combination* of phosphorus inversion and Pt−P rotation. We cannot determine the relative contributions from each of these processes to the overall barriers, but we conclude that phosphorus inversion in these complexes has a *maximum* barrier of ca. 11−13 kcal/mol. A referee called this conclusion and those of the accompanying article "intrinsically flawed since the inversion process is coupled with rotation about the Pt−PRR′ bond. This arises due to the fact that these systems contain cis-bidentate diphosphine ligands in a square-planar array". However, this problem is not unique to square planar systems; it also arises in, for example, octahedral[1c] and pseudo-tetrahedral (three-legged piano stool)[1a,b] phosphido complexes. The referee also commented that "all of the data are not definitive unless the assumption that rotation is barrierless is made". In our view, the importance of these results is not the exact value of the phosphorus inversion barriers, but the fact that they are so much lower than the ones observed in tertiary phosphines. We cannot determine if rotation occurs through the pyramidal or the planar form of the phosphido ligand. It may, however, be possible to obtain "pure" inversion barriers in related systems by restricting the rotation of metal phosphido ligands.

Why are inversion barriers in these platinum(II) phosphido complexes and the ones reported in the accompanying article so low? Our previously reported X-ray structures of platinum(II) phosphido complexes confirm that the geometry at phosphorus is pyramidal.[4] The transition state for pyramidal inversion presumably includes a trigonal planar phosphido P with a lone pair in a p-orbital. For inversion barriers to be low, the energy difference between the planar transition state and the pyramidal ground state must be relatively small.

The barrier to pyramidal inversion in tertiary phosphines is greatly reduced by the presence of an electropositive substituent on phosphorus.[18] For example, the inversion barriers in P(Ph)(*i*-Pr)(EMe_3) (E = Si, Ge, Sn) are at least 10 kcal/mol lower than the inversion barrier in P(Ph)(Me)(CMe_3). Mislow and co-workers suggested that the electropositive Si, Ge, and Sn substituents increase s-character in the P−E bond, which results in a concomitant increase in the p-character of the lone

(16) Alternatively, slow Pt−P rotation, which prevents the PPh_2 group from entering the square plane, would make the CF_2 fluorines inequivalent even if inversion were fast on the NMR time scale.

(17) Restricted rotation around the Pt−phosphido bond may also account for the dynamic process that is apparent in the low-temperature ^{31}P NMR spectrum of Pt(dppe)(Me)(PPhIs) (**2**).

(18) Baechler, R. D.; Mislow, K. *J. Am. Chem. Soc.* **1971**, *93*, 773−774.

Chart 2

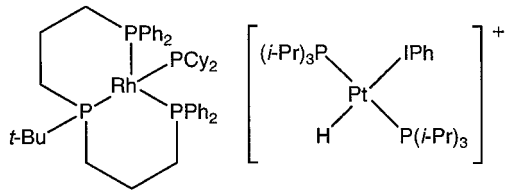

pair. Since the lone pair occupies an orbital of essentially pure p-character in the planar transition state, the energy difference between the ground state and the transition state is reduced.[19] Although Pt(II) is an electropositive substituent, our crystallographic and ^{31}P NMR results are consistent with *low* s-character in the Pt−P bonds. This should lead to a high inversion barrier, due to the rehybridization energy necessary to reach the sp^2 transition state.

Low inversion barriers in early metal transition metal phosphido complexes are often rationalized in terms of stabilization of the planar transition state by donation of the lone pair of electrons to an empty d-orbital on the metal. For example, the X-ray structure of Hf(Cp)$_2$(PEt$_2$)$_2$ shows two distinct bonding modes for the Hf−PEt$_2$ ligand.[1f] One is pyramidal with a Hf−PEt$_2$ bond length of 2.682(1) Å, and the other is planar with a Hf−PEt$_2$ bond length of 2.488(1) Å. The room-temperature ^{31}P NMR spectra for a series of Hf and Zr complexes show a singlet, consistent with rapid interconversion of the pyramidal and planar phosphido ligands, and the barrier to phosphido interconversion in Hf(Cp)$_2$(PCy$_2$)$_2$ was found to be 6.0 ± 0.2 kcal/mol. A theoretical study for a series of Ti(IV) phosphido complexes also cites phosphido to metal π-interaction as an important contribution to stabilization of the planar transition state in early metal phosphido complexes.[1j]

However, stabilization of the planar transition state through interaction of the phosphido lone pair with d-orbitals on the metal cannot be invoked in these d^8 Pt(II) complexes, as the metal d-orbitals of appropriate symmetry are filled. In fact, compared to other transition metal phosphido complexes, one might expect Pt(II) phosphido complexes to show increased inversion barriers due to unfavorable interactions between filled d-orbitals on platinum and the lone pair of electrons on phosphorus. This type of unfavorable metal−ligand antibonding π-interaction has been suggested to explain the lack of terminal oxo complexes of the late transition metals.[20]

However, in the related d^8 Rh(I) terminal phosphido complex Rh(bupp$_2$Ph$_4$)(PCy$_2$) (Chart 2, bupp$_2$Ph$_4$ = (*t*-Bu)P(CH$_2$CH$_2$CH$_2$PPh$_2$)$_2$; Cy = cyclo-C$_6$H$_{11}$), based on the ^{31}P NMR chemical shift of the phosphido ligand (δ 186) and the large J_{Rh-P} (154 Hz) as compared to the diphenylphosphido complex Rh(bupp$_2$Ph$_4$)(PPh$_2$) (δ 26, J_{Rh-P} = 92 Hz), Dahlenburg et al. suggested some degree of Rh−P double-bond character.[21] A Rh(p$_z$)−P(p) π-interaction was proposed on the basis of MO calculations for the square planar model complex Rh(PH$_3$)$_3$(PH$_2$) with an sp^2-hybridized phosphido ligand in the RhL$_3$ plane.

A similar bonding picture has been invoked for iodide-to-platinum π-bonding in the Pt(II) cation [Pt(P(*i*-Pr)$_3$)$_2$(H)(η^1-IPh)][BAr$_f$] (Chart 2, BAr$_f$ = B(3,5-(CF$_3$)$_2$C$_6$H$_3$)$_4$).[22] Kubas and co-workers proposed a π-bonding interaction between the iodide lone pair in a p$_z$-orbital and a Pt MO formed by mixing of the filled Pt(d$_{yz}$) orbital and the empty Pt(p$_z$) orbital.[23] This interaction was proposed to outweigh the filled Pt(d$_{yz}$)−iodide lone pair repulsion to give a net stabilization of about 10 kcal/mol and overcome steric repulsion between the phenyl and isopropyl groups, which are unusually close in the solid state. It was further suggested that the iodide lone pair electrons are able to interact favorably with Pt(II) p- and d-orbitals because they are higher in energy than those of analogous alkoxide, hydroxide, or amido ligands and are, thereby, better suited for overlap with these Pt(II) orbitals.

In our system, a similar interaction between the phosphorus lone pair and the d$_{yz}$- and p$_z$-orbitals of Pt(II) may be responsible for planar transition state stabilization and, consequently, the reduced inversion barriers observed for these perfluoroacyl phosphido complexes.

Conclusion

We prepared Pt(dppe)(R)(PPhR′) complexes that contain either diastereotopic methyl groups on the phosphido substituent or diastereotopic CF$_2$ fluorines on a Pt-bound perfluoroacyl ligand. NMR analysis of Pt(dppe)(Me)(PPh*i*-Bu) (**1**) and Pt(dppe)(Me)(PPhIs) (**2**) was inconclusive, but dynamic behavior was observed for the complexes Pt(dppe)(COC$_3$F$_7$)(PPhAr) (**11**−**15**). The fluxional behavior in the perfluoroacyl complexes **11**−**15** is consistent with the operation of two dynamic processes: rotation around the Pt−phosphido bond and inversion at the phosphido phosphorus. To explain the observed NMR data, both processes must be fast at room temperature in complexes **11**−**15**. Therefore, we conclude that the calculated energy barriers (ca. 11−13 kcal/mol) for these processes provide an upper limit for the barrier to pyramidal inversion in these complexes, consistent with phosphido inversion barriers calculated for other transition metal phosphido complexes. The reduced inversion barriers in these Pt(II) complexes may be explained by interaction of the phosphido lone pair with the d$_{yz}$ and p$_z$ platinum orbitals, which could lower the energy of the planar transition state relative to the pyramidal ground state.

Experimental Section

General Details. Unless otherwise noted, all reactions and manipulations were performed in dry glassware under a nitrogen atmosphere at 20 °C in a drybox or using standard Schlenk techniques. Petroleum ether (bp 38−53 °C), ether, THF, and toluene were dried and distilled before use from Na/benzophenone. CH$_2$Cl$_2$ and acetonitrile were distilled from CaH$_2$.

Unless otherwise noted, all NMR spectra were recorded on a Varian 300 MHz spectrometer. ^{1}H and ^{13}C NMR chemical

(19) Mislow, K. *Trans. N. Y. Acad. Sci.* **1973**, *35*, 227−242.
(20) Mayer, J. M. *Comments Inorg. Chem.* **1988**, *8*, 125−135.
(21) Dahlenburg, L.; Hock, N.; Berke, H. *Chem. Ber.* **1988**, *121*, 2083−2093.
(22) Butts, M. D.; Scott, B. L.; Kubas, G. J. *J. Am. Chem. Soc.* **1996**, *118*, 11831−11843.
(23) Dahlenburg and co-workers (ref 21) include similar mixing with a d-orbital of this symmetry, but use a slightly different coordinate system.

shifts are reported relative to Me_4Si and were determined by reference to the residual ^1H or ^{13}C solvent peaks. ^{31}P NMR chemical shifts are reported relative to H_3PO_4 (85%) used as an external reference. ^{19}F NMR chemical shifts are reported relative to $CFCl_3$ used as an external reference. Unless otherwise noted, peaks in NMR spectra are singlets. Coupling constants are reported in hertz. Infrared spectra were recorded using KBr pellets on a Perkin-Elmer 1600 series FTIR machine. Elemental analyses were provided by Schwarzkopf Microanalytical Laboratory. Unless otherwise noted, reagents were from commercial suppliers. The following compounds were made by the literature procedures: Pt(dppe)(Me)(OMe),[3] PHPhIs,[5] $Pt(PPh_2Me)_4$,[7] PHP*o*-anisyl,[24] PH(Ph)(Mes).[25]

Pt(dppe)(Me)(PPhIs) (2). To a stirred slurry of Pt(dppe)(Me)(OMe) (98 mg, 0.15 mmol) in THF (5 mL) was added PHPhIs (57 mg, 0.18 mmol) in THF (2 mL). The reaction mixture immediately became homogeneous, and the color turned bright orange. The solvent was removed under vacuum, and the yellow residue was washed twice with petroleum ether (2 mL portions). The solid was dried and dissolved in a minimum amount of THF. The THF solution was filtered, and petroleum ether was added. Cooling of this solution to −25 °C overnight gave 92 mg (65%) of a yellow solid. ^1H NMR (toluene-d_8): δ 7.57−7.52 (m, 8H, Ar), 7.22−7.16 (m, 4H, Ar), 7.05−6.99 (m, 12H, Ar), 6.74−6.68 (m, 3H, Ar), 4.79−4.68 (m, 2H, *o*-C*H*Me_2), 2.85 (septet, $^3J_{HH}$ = 7, 1H, *p*-C*H*Me_2), 1.86−1.76 (m, 4H, dppe CH_2), 1.27 (d, $^3J_{HH}$ = 7, 6H, *p*-CH*Me*$_2$), 1.21 (d, $^3J_{HH}$ = 7, 12H, *o*-CH*Me*$_2$), 0.89−0.83 (m, $^2J_{Pt-H}$ = 67, 3H, Pt-Me). $^{13}C\{^1H\}$ NMR (toluene-d_8): δ 155.3−155.1 (m, quat. Ar), 147.7 (quat. Ar), 133.8−133.1 (m, Ar), 132.9 (quat. Ar), 132.4 (quat. Ar), 132.0 (quat. Ar), 131.5 (quat. Ar), 130.5 (Ar), 130.1 (Ar), 128.6 (Ar), 128.5 (Ar), 128.3 (Ar), 128.2 (Ar), 126.6−126.5 (m, Ar), 125.4 (quat. Ar), 125.1 (quat. Ar), 124.7 (quat. Ar), 123.3 (Ar), 121.3−121.2 (m, Ar), 34.6 (*p*-*C*HMe$_2$), 33.9 (d, $^3J_{PC}$ = 17, *o*-*C*HMe$_2$), 32.6−31.9 (m, dppe CH_2), 29.5−28.9 (m, dppe CH_2), 25.7 (*o*-CH*Me*$_2$), 24.4 (*p*-CH*Me*$_2$), 2.7 (dd, $^2J_{PC}$ = 83, 8, Pt−Me, Pt satellites were not resolved). $^{31}P\{^1H\}$ NMR (toluene-d_8): δ 49.3 (d, $^2J_{PP}$ = 174, $^1J_{Pt-P}$ = 1969, P trans to PPhIs), 45.4 ($^1J_{Pt-P}$ = 1915, P trans to Me), −25.3 (d, $^2J_{PP}$ = 174, $^1J_{Pt-P}$ = 1118, PPhIs). IR: 3055, 2955, 2866, 1483, 1461, 1427, 1383, 1305, 1183, 1100, 1016, 877, 822, 744, 694, 644, 533, 488 cm^{-1}. Anal. Calcd for $C_{48}H_{55}P_3Pt$: C, 62.66; H, 6.04. Found: C, 62.10; H, 5.72.

***trans*-Pt(PPh_2Me)$_2$(COC_3F_7)(Cl) (3).** To a stirred suspension of $Pt(PPh_2Me)_4$ (656 mg, 0.656 mmol, recrystallized from toluene/petroleum ether at −25 °C) in petroleum ether (80 mL) was added dropwise a solution of C_3F_7COCl (300 μL, 2.01 mmol, distilled) in petroleum ether (5 mL) over a period of 15 min. The reaction mixture was allowed to stir at room temperature for 2 h, during which time the bright yellow solid gradually turned white. The solvent was removed via cannula filter, and the white solid was washed twice with petroleum ether (20 mL portions). Recrystallization from THF/petroleum ether at −25 °C gave 418 mg (77%) of product as a white solid. Further recrystallization from CH_2Cl_2/EtOH/ether gave crystals suitable for X-ray diffraction. ^1H NMR ($CDCl_3$): δ 7.70 (broad, 8H, Ar), 7.44 (12H, Ar), 2.17 (apparent t, J = 4, $^3J_{Pt-H}$ = 32, 6H, P−Me). $^{31}P\{^1H\}$ NMR ($CDCl_3$): δ 6.5 (t, $^2J_{PF}$ = 5, $^1J_{Pt-P}$ = 2916). ^{19}F NMR ($CDCl_3$): δ −81.2 (t, J_{FF} = 9, CF_3), −111.5 to −111.6 (m, COC*F*$_2$CF$_2$), −127.6 to −127.7 (m, COCF$_2$C*F*$_2$). IR: 3057, 2920, 1691, 1672 (C═O), 1485, 1436, 1334, 1209, 1183, 1105, 894, 734, 692, 659, 505, 487, 456 cm^{-1}. Anal. Calcd for $C_{30}H_{26}ClF_7OP_2Pt$: C, 43.51; H, 3.17. Found: C, 43.35; H, 3.17.

Pt(dppe)(COC_3F_7)(Cl) (4). To a stirred solution of *trans*-Pt(PPh_2Me)$_2$(COC_3F_7)(Cl) (350 mg, 0.423 mmol) in THF (10 mL) was added a solution of dppe (202 mg, 0.507 mmol) in THF (5 mL). The reaction mixture immediately turned yellow. The solvent was removed under vacuum, and the yellow residue was washed twice with petroleum ether (5 mL portions). The solid was dissolved in CH_2Cl_2 and filtered, and ether was added. Cooling of this solution to −25 °C overnight yielded 245 mg (70%) of product. Subsequent recrystallization from CH_2Cl_2/ether gave crystals suitable for X-ray diffraction. ^1H NMR (CD_2Cl_2): δ 7.87−7.80 (m, 4H, Ar), 7.73−7.67 (m, 4H, Ar), 7.55−7.47 (m, 12H, Ar), 2.54−2.40 (m, 2H, dppe CH_2), 2.18−2.02 (m, 2H, dppe CH_2). $^{13}C\{^1H\}$ NMR (CD_2Cl_2): δ 134.0−133.4 (m, Ar), 132.5−132.4 (m, quat. Ar), 131.9−131.8 (m, quat. Ar), 129.6−128.9 (m, Ar), 127.5 (quat. Ar), 126.7 (quat. Ar), 31.8−31.1 (m, dppe CH_2), 24.9−24.4 (m, dppe CH_2). The carbons of the COC_3F_7 ligand were not resolved. IR: 3059, 2916, 1662 (C═O), 1482, 1435, 1339, 1225, 1201, 1177, 1106, 876, 825, 747, 716, 706, 690, 535 cm^{-1}. Anal. Calcd for $C_{30}H_{24}ClF_7OP_2Pt$: C, 43.62; H, 2.93. Found: C, 43.51; H, 2.92.

[Pt(dppe)(COC_3F_7)(NCMe)][BF_4] (5). To a slurry of Pt(dppe)(COC_3F_7)(Cl) (300 mg, 0.363 mmol) in THF (5 mL) and CH_3CN (3 mL) was added $AgBF_4$ (71 mg, 0.36 mmol) in CH_3CN (2 mL). Immediate formation of AgCl occurred as indicated by a white precipitate. The reaction mixture was stirred vigorously overnight. The cloudy gray reaction mixture was filtered through a fine frit with Celite to give a yellow filtrate. The solvent was removed under vacuum, and the pale yellow residue was washed with petroleum ether (three 5 mL portions) and dried to give 305 mg (91%) of crude product, which was pure enough to use in subsequent reactions. A sample for elemental analysis was recrystallized first from THF/petroleum ether at −25 °C and then from CH_2Cl_2/ether at −25 °C to give a yellow powder. ^1H NMR ($CDCl_3$): δ 7.34−7.16 (broad m, 20H, Ar), 2.43−2.31 (m, 2H, dppe CH_2), 2.14−1.98 (m, 2H, dppe CH_2), 2.00 (3H, NCMe). IR: 3055, 2933, 2300 (CN), 1672 (C═O), 1483, 1439, 1411, 1339, 1205, 1111, 1061 (BF_4), 822, 750, 711, 688, 533, 489 cm^{-1}. Anal. Calcd for $C_{32}H_{27}NBF_{11}OP_2Pt$: C, 41.85; H, 2.96; N, 1.53. Found: C, 41.19; H, 2.96; N, 1.33.

[Pt(dppe)(COC_3F_7)(PHPhMes)][BF_4] (6). To a solution of [Pt(dppe)(COC_3F_7)(NCMe)][BF_4] (263 mg, 0.286 mmol) in THF (5 mL) was added PHPhMes (73 mg, 0.32 mmol) in THF (2 mL). The reaction mixture turned slightly darker yellow, and the solvent was removed under vacuum. The yellow residue was washed twice with petroleum ether (3 mL portions) and dried to give 305 mg (96%) of crude product. Double recrystallization from THF/petroleum ether at −25 °C gave analytically pure light yellow powder. ^1H NMR (CD_2Cl_2): δ 7.83−7.35 (broad m, 22H, Ar), 7.38−7.17 (m, 4H, Ar), 7.09 (dm, $^1J_{PH}$ = 390, 1H, P−H), 6.82 (2H, Ar), 2.70−2.17 (m, 4H, dppe CH_2), 2.32 (6H, *o*-Me), 2.25 (3H, *p*-Me). IR: 3055, 2922, 2322 (w, P−H), 1672 (C═O), 1483, 1433, 1411, 1377, 1333, 1227, 1205, 1055 (BF_4), 1000, 883, 850, 816, 744, 694, 533, 483 cm^{-1}. Anal. Calcd for $C_{45}H_{41}BF_{11}OP_3Pt$: C, 48.89; H, 3.74. Found: C, 49.06; H, 3.66.

[Pt(dppe)(COC_3F_7)(PHP*o*-anisyl)][BF_4] (7). To a solution of [Pt(dppe)(COC_3F_7)(NCMe)][BF_4] (266 mg, 0.290 mmol) in THF (3 mL) was added PHP*o*-anisyl (69 mg, 0.32 mmol) in THF (2 mL). The solvent was removed under vacuum. The pale yellow residue was washed twice with petroleum ether (3 mL portions) and dried to give 266 mg (84%) of crude product. Recrystallization from THF/petroleum ether at −25 °C gave analytically pure off-white powder. ^1H NMR (CD_2Cl_2): δ 7.75−7.51 (m, 14H, Ar), 7.44−7.35 (m, 7H, Ar), 7.31−7.25 (m, 5H, Ar), 6.97−6.93 (m, 1H, Ar), 6.83−6.79 (m, 1H, Ar), 6.65−6.58 (m, 1H, Ar), 6.39 (dm, $^1J_{PH}$ = 410, 1H, P−H), 4.03 (3H, OMe), 2.71−2.34 (m, 4H, dppe CH_2). IR: 3051, 2354 (w, P−H), 1670 (C═O), 1474, 1436, 1338, 1278, 1218, 1060 (BF_4), 907, 869, 820, 749, 695, 537, 488 cm^{-1}. Anal. Calcd for $C_{43}H_{37}BF_{11}O_2P_3Pt$: C, 47.23; H, 3.41. Found: C, 47.46; H, 3.25.

[Pt(dppe)(COC_3F_7)(PHPhIs)][BF_4] (8). To a stirred solution of Pt(dppe)(COC_3F_7)(Cl) (177 mg, 0.214 mmol) and PHPhIs

(24) Vedejs, E.; Donde, Y. *J. Am. Chem. Soc.* **1997**, *119*, 9293−9294.
(25) Wicht, D. K.; Kourkine, I. V.; Kovacik, I.; Glueck, D. S.; Concolino, T. E.; Yap, G. P. A.; Incarvito, C. D.; Rheingold, A. L. *Organometallics*, accepted for publication.

(74 mg, 0.24 mmol) in CH_2Cl_2 (5 mL) was added $AgBF_4$ (42 mg, 0.21 mmol) in CH_3CN (2 mL). Immediate formation of AgCl was observed, and the reaction mixture was stirred vigorously for 30 min at room temperature. Filtration and removal of solvent under vacuum gave a yellow residue. The solid was washed twice with petroleum ether (3 mL portions) and dissolved in THF. The solution was filtered, and petroleum ether was added. Cooling of this solution to −25 °C overnight gave 215 mg (84%) of product. ^{1}H NMR ($CDCl_3$): δ 7.96−7.92 (m, 2H, Ar), 7.81−7.31 (m, 15H, Ar), 7.24−7.01 (m, 8H, Ar), 6.93−6.91 (m, 2H, Ar), 6.76 (dm, $^1J_{PH}$ = 388, 1H, P−H), 2.97−2.93 (m, 3H, dppe CH_2 and *p*-C*H*Me$_2$), 2.86−2.79 (m, 2H, *o*-C*H*Me$_2$), 2.37−2.30 (m, 2H, dppe CH_2), 1.17 (d, $^3J_{HH}$ = 7, 6H, *p*-CH*Me*$_2$), 0.95 (d, $^3J_{HH}$ = 7, 6H, *o*-CH*Me*$_2$), 0.76 (broad, 6H, *o*-CH*Me*$_2$). ^{13}C{^{1}H} NMR ($CDCl_3$): δ 153.6−153.5 (m, quat. Ar), 152.6−152.5 (m, quat. Ar), 134.6−134.4 (m, Ar), 133.9−133.6 (m, Ar), 133.3−133.1 (m, Ar), 132.4−132.1 (m, Ar), 131.7−131.6 (m, Ar), 130.0−129.8 (m, Ar), 129.4−129.0 (m, Ar), 127.0−124.3 (m, quat. Ar), 123.1−122.9 (m, Ar), 117.8−117.7 (m, quat. Ar), 117.0−116.9 (m, quat. Ar), 34.2 (*p*-*C*HMe$_2$), 33.6 (*o*-*C*HMe$_2$), 33.5 (*o*-*C*HMe$_2$), 27.8−26.8 (m, dppe CH_2), 24.2 (*p*-CH*Me*$_2$), 23.6 (*o*-CH*Me*$_2$), 23.5 (*o*-CH*Me*$_2$). The carbons of the COC_3F_7 ligand were not resolved. IR: 3044, 2955, 2866, 2322 (w, P−H), 1672 (C═O), 1483, 1463, 1437, 1336, 1227, 1208, 1184, 1105, 1057 (BF_4), 998, 879, 822, 746, 706, 692, 531, 484 cm^{-1}. Anal. Calcd for $C_{51}H_{53}BF_{11}OP_3Pt$·THF: C, 52.34; H, 4.88. Found: C, 52.49; H, 4.61. The presence of THF in the analytical sample was confirmed by ^{1}H NMR.

Synthesis of PHPhMes-F$_9$ and [Pt(dppe)(COC$_3$F$_7$)(PHPhMes-F$_9$)][BF$_4$] (9). LiMes-F_9 was prepared according to the reported procedure,[26] and the secondary phosphine was prepared by a modification of the procedure for PH_2Mes-F_9.[27] To a Schlenk flask containing 2,4,6-tris(trifluoromethyl)-benzene (3.23 g, 11.4 mmol) in ether (10 mL) was transferred *n*-BuLi (7.9 mL, 1.6 M in hexanes, 12.6 mmol) dropwise via cannula. The addition was done over a period of 30 min at room temperature, and the cloudy yellow solution was stirred for an additional 30 min. A flask containing $PPhCl_2$ (1.7 mL, 12.6 mmol) in ether (15 mL) was fitted with an addition funnel, and the LiMes-F_9 solution was transferred to the addition funnel via cannula. The $PPhCl_2$ solution was cooled to −78 °C with a dry ice/acetone bath, and the lithium reagent was added to this solution dropwise over a period of 45 min. The reaction mixture was warmed to room temperature, and the solution was filtered. The remaining LiCl was washed with ether (20 mL), and the filtrates were combined. The PClPhMes-F_9 solution was transferred via cannula to a cold (dry ice/acetone) gray slurry of $LiAlH_4$ (836 mg, 22.9 mmol) in ether (20 mL). The cold bath was removed, and the reaction mixture was stirred at room temperature for 1 h. The reaction was carefully quenched with degassed, distilled water, and then an additional 40 mL of H_2O was added. The ether layer was filtered off, and the aqueous layer was washed twice with ether (20 mL portions). The combined ether layers were dried over $MgSO_4$. ^{31}P NMR showed the desired product and phenylphosphine (caution, STENCH). The ether and phenylphosphine were removed under vacuum to give a brownish oil. Degassed 2-propanol was added, and the yellow solution was cooled to −25 °C to give 1.04 g (23%) of PH(Ph)Mes-F_9 as a white solid in two crops. ^{1}H NMR (C_6D_6): δ 7.84 (2H, Ar), 7.17−7.12 (m, 2H, Ar), 7.00−6.69 (m, 3H, Ar), 5.73 (d septet, $^1J_{PH}$ = 234, $^5J_{HF}$ = 4, P−H). ^{31}P{^{1}H} NMR (C_6D_6): δ −59.0 (septet, $^4J_{PF}$ = 27 Hz). ^{31}P NMR (C_6D_6): δ −59 (dm, $^1J_{PH}$ = 234). ^{19}F NMR (C_6D_6): δ −58.0 (dd, $^4J_{PF}$ = 27, $^5J_{HF}$ = 4, *o*-CF_3), −63.7 (*p*-CF_3).

To a solution of [Pt(dppe)(COC_3F_7)(NCMe)][BF_4] (176 mg, 0.192 mmol) in THF (3 mL) was added PHPhMes-F_9 (82 mg, 0.21 mmol) in THF (2 mL). The solvent was removed under vacuum. The yellow residue was washed twice with petroleum ether (3 mL portions) and three times with ether (2 mL portions) until the sticky solid became completely insoluble in ether. Recrystallization from CH_2Cl_2/ether at −25 °C gave 162 mg (67%) of product. ^{1}H NMR (CD_2Cl_2): δ 8.28−8.15 (broad m, 2H, Ar), 8.01−7.94 (m, 2H, Ar), 7.78−7.24 (m, 23H, Ar), 7.22 (broad d, $^1J_{PH}$ = 400, 1H, P−H), 2.81−2.41 (m, 4H, dppe CH_2). IR: 3055, 2322 (w, P−H), 1677 (C═O), 1627, 1583, 1483, 1433, 1338, 1283, 1200, 1061 (BF_4), 916, 872, 855, 816, 744, 694, 533, 483 cm^{-1}. Anal. Calcd for $C_{45}H_{32}BF_{20}OP_3Pt$: C, 42.64; H, 2.55. Found: C, 42.85; H, 2.50.

[Pt(dppe)(COC$_3$F$_7$)(PHPh$_2$)][BF$_4$] (10). To a solution of [Pt(dppe)(COC_3F_7)(NCMe)][BF_4] (176 mg, 0.192 mmol) in THF (3 mL) was added $PHPh_2$ (37 μL, 0.21 mmol) via microliter syringe. The solvent was removed under vacuum. The pale yellow solid was washed twice with petroleum ether (2 mL portions) and dried to yield 167 mg (82%) of crude product. Double recrystallization from THF/petroleum ether at −25 °C gave analytically pure light yellow powder. ^{1}H NMR (CD_2Cl_2): δ 7.72−7.26 (m, 30H, Ar), 6.33 (dm, $^1J_{PH}$ = 395, 1H, P−H), 2.70−2.33 (m, 4H, dppe CH_2). IR: 3055, 2343 (w, P−H), 1672 (C═O), 1483, 1438, 1339, 1216, 1105, 1050 (BF_4), 927, 905, 861, 822, 744, 700, 527, 477 cm^{-1}. Anal. Calcd for $C_{42}H_{35}BF_{11}OP_3Pt$: C, 47.43; H, 3.32. Found: C, 47.56; H, 3.19.

Pt(dppe)(COC$_3$F$_7$)(PPhMes) (11). To a solution of [Pt(dppe)(COC_3F_7)(PHPhMes)][BF_4] (300 mg, 0.271 mmol) in THF (5 mL) was added LiN($SiMe_3$)$_2$ (55 mg, 0.33 mmol) in THF (3 mL). Alternatively, the phosphine complex could be generated in situ by the addition of PHPhMes to [Pt(dppe)(COC_3F_7)(NCMe)][BF_4] as described, identified spectroscopically, and treated with base directly. The solvent was removed under vacuum, and the yellow residue was washed with petroleum ether (three 2 mL portions). The yellow solid was extracted with ca. 50 mL of toluene and filtered through a fine frit with Celite. The filtrate was concentrated to ca. 10 mL, and petroleum ether was added. Cooling of this solution to −25 °C gave 190 mg (69%) of product in two crops. ^{1}H NMR (THF-d_8): δ 7.74 (broad, 3H, Ar), 7.63−7.57 (m, 4H, Ar), 7.46−7.16 (m, 13H, Ar), 6.89−6.88 (m, 2H, Ar), 6.89−6.63 (m, 3H, Ar), 6.45 (2H, Ar), 2.44 (6H, *o*-Me), 2.36−2.24 (m, 2H, dppe CH_2), 2.18−2.05 (m, 2H, dppe CH_2), 2.10 (3H, *p*-Me). IR: 3055, 2922, 1661 (C═O), 1572, 1483, 1433, 1333, 1227, 1205, 1105, 1027, 1000, 883, 850, 822, 744, 694, 527, 483 cm^{-1}. Anal. Calcd for $C_{45}H_{40}F_7OP_3Pt$: C, 53.10; H, 3.97. Found: C, 53.27; H, 4.03.

Pt(dppe)(COC$_3$F$_7$)(PPh*o*-anisyl) (12). To a solution of [Pt(dppe)(COC_3F_7)(PHPh*o*-anisyl)][BF_4] (225 mg, 0.206 mmol) in THF (8 mL) was added LiN($SiMe_3$)$_2$ (38 mg, 0.23 mmol) in THF (5 mL). The reaction mixture immediately turned bright yellow, and the solvent was removed under vacuum. The yellow residue was extracted with toluene (20 mL) and filtered through a fine frit with Celite. The filtrate was concentrated to a volume of ∼3 mL, and petroleum ether was added. Cooling of this solution overnight at −25 °C gave 100 mg (45%) of bright yellow powder in two crops. Recrystallization from THF/petroleum ether at −25 °C gave a sample for analysis. ^{1}H NMR (THF-d_8): δ 7.68 (broad, 6H, Ar), 7.41−7.21 (broad m, 16H, Ar), 6.86−6.71 (m, 5H, Ar), 6.55−6.53 (m, 1H, Ar), 6.37−6.33 (m, 1H, Ar), 3.85 (3H, OMe), 2.44−2.14 (m, 4H, dppe CH_2). IR: 3052, 1648 (C═O), 1577, 1463, 1436, 1338, 1267, 1229, 1202, 1104, 1027, 880, 815, 744, 695, 531, 488 cm^{-1}. Anal. Calcd for $C_{43}H_{36}F_7O_2P_3Pt$: C, 51.35; H, 3.62. Found: C, 51.20; H, 3.90.

Pt(dppe)(COC$_3$F$_7$)(PPhIs) (13). To a stirred suspension of [Pt(dppe)(COC_3F_7)(PHPhIs)][BF_4] (358 mg, 0.301 mmol) in THF (10 mL) was added LiN($SiMe_3$)$_2$ (61 mg, 0.36 mmol) in THF (5 mL). The reaction mixture immediately became bright orange and was allowed to stir at room temperature for 15 min. The solvent was removed under vacuum, and the yellow-orange residue was washed three times with petroleum ether (5 mL portions). The solid was extracted with 20 mL of toluene

(26) Carr, G. E.; Chambers, R. D.; Holmes, J. F.; Parker, D. G. *J. Organomet. Chem.* **1987**, *325*, 13−23.
(27) Schollz, M.; Roesky, H. W.; Stalke, D.; Keller, K.; Edelmann, F. T. *J. Organomet. Chem.* **1989**, *366*, 73−85.

and filtered through a fine frit with Celite. The bright orange filtrate was concentrated to 5 mL, and petroleum ether was added. Cooling of this solution to −25 °C gave 237 mg (71%) of bright yellow product. ^{1}H NMR (toluene-d_8): δ 7.67−7.61 (m, 4H, Ar), 7.53−7.47 (m, 4H, Ar), 7.36−7.32 (m, 2H, Ar), 7.14−6.91 (m, 14H, Ar), 6.73−6.71 (m, 3H, Ar), 4.72−4.67 (m, 2H, *o*-C*H*Me$_2$), 2.79 (septet, $^3J_{HH}$ = 7, 1H, *p*-C*H*Me$_2$), 1.87−1.57 (m, 4H, dppe CH_2), 1.24 (d, $^3J_{HH}$ = 7, 6H, *p*-CH*Me$_2$*), 1.19 (broad d, $^3J_{HH}$ = 6, 12H, *o*-CH*Me$_2$*). ^{13}C{^{1}H} NMR (toluene-d_8): δ 154.9−154.7 (m, quat. Ar), 148.3 (quat. Ar), 146.6−146.2 (m, quat. Ar), 136.6 (quat. Ar), 136.3 (quat. Ar), 135.2 (Ar), 134.9 (Ar), 134.0−133.7 (m, Ar), 131.5 (quat. Ar), 131.2 (Ar), 130.9 (quat. Ar), 130.5 (Ar), 128.8 (Ar), 128.7 (Ar), 128.3 (Ar), 128.2 (Ar), 126.6−126.5 (m, Ar), 125.4 (quat. Ar), 125.1 (quat. Ar), 124.7 (Ar), 121.6−121.5 (m, Ar), 34.5 (*p*-*C*HMe$_2$), 34.1 (d, $^3J_{PC}$ = 17, *o*-*C*HMe$_2$), 29.5−28.8 (m, dppe CH_2), 25.8 (*o*-CH*Me$_2$*), 24.2 (*p*-CH*Me$_2$*). IR: 3054, 2957, 2865, 1651 (C═O), 1579, 1482, 1462, 1436, 1414, 1335, 1225, 1204, 1104, 1026, 879, 823, 742, 694, 650, 594, 529, 484 cm^{-1}. Anal. Calcd for $C_{51}H_{52}F_7OP_3Pt$: C, 55.58; H, 4.77. Found: C, 55.66; H, 4.97.

Pt(dppe)(COC$_3$F$_7$)(PPhMes-F$_9$) (14). To a solution of [Pt(dppe)(COC$_3$F$_7$)(PHPhMes-F$_9$)][BF$_4$] (224 mg, 0.177 mmol) in THF (5 mL) was added LiN(SiMe$_3$)$_2$ (30 mg, 0.18 mmol) in THF (3 mL). Alternatively, the phosphine complex could be generated in situ by the addition of PHPhMes-F$_9$ to [Pt(dppe)(COC$_3$F$_7$)(NCMe)][BF$_4$] as described, identified spectroscopically, and treated with base directly. The solvent was removed under vacuum to give a dark orange residue. The residue was extracted with toluene (∼10 mL) and filtered through a fine frit with Celite. The solvent was removed under vacuum, and the orange residue was dissolved in ether. The ether solution was filtered and concentrated under vacuum to a volume of ∼3 mL. Petroleum ether was added, and cooling of this solution to −25 °C overnight gave 148 mg (71%) of orange-red product. ^{1}H NMR (toluene-d_8): δ 8.05 (2H, Ar), 7.51 (broad, 6H, Ar), 7.41−7.36 (m, 3H, Ar), 7.05 (broad, 6H, Ar), 6.90 (broad, 6H, Ar), 6.78−6.65 (m, 4H, Ar), 1.82−1.61 (m, 4H, dppe CH_2). IR: 3055, 1661 (C═O), 1572, 1483, 1433, 1366, 1333, 1277, 1189, 1133, 1072, 1028, 905, 883, 861, 822, 744, 700, 533, 483, 433 cm^{-1}. Anal. Calcd for $C_{45}H_{31}F_{16}OP_3Pt$: C, 45.81; H, 2.65. Found: C, 45.40; H, 2.65.

Pt(dppe)(COC$_3$F$_7$)(PPh$_2$) (15). To a solution of [Pt(dppe)(COC$_3$F$_7$)(PHPh$_2$)][BF$_4$] (142 mg, 0.134 mmol) in THF (3 mL) was added LiN(SiMe$_3$)$_2$ (25 mg, 0.15 mmol) in THF (2 mL). The reaction mixture immediately became bright yellow, and the solvent was removed under vacuum. The yellow residue was washed three times with petroleum ether (1 mL portions) and dried. The yellow solid was extracted with toluene (20 mL) and filtered through a fine frit with Celite. The filtrate was concentrated to a volume of ∼2 mL, and petroleum ether was added. Cooling of this solution overnight at −25 °C gave 79 mg (61%) of product in two crops. ^{1}H NMR (THF-d_8): δ 7.62−7.23 (broad m, 9H, Ar), 7.10−6.71 (broad m, 21H, Ar), 1.91−1.58 (m, 4H, dppe CH_2). IR: 3055, 1655 (C═O), 1483, 1433, 1333, 1228, 1205, 1111, 1027, 994, 877, 822, 744, 694, 527, 483 cm^{-1}. Anal. Calcd for $C_{42}H_{34}F_7OP_3Pt$: C, 51.70; H, 3.52. Found: C, 51.77; H, 3.81.

Variable-Temperature NMR Data. The reported temperatures were calibrated from the chemical shift difference of the signals in the ^{1}H NMR spectrum of a standard sample of methanol (temperatures < 20 °C) or ethylene glycol (temperatures > 20 °C). The uncertainty in the $\Delta G^{\ddagger}(T_c)$ values was estimated on the basis of the assumption that there is an error of ±10 °C in the determination of the coalescence temperature.

Crystallographic Structural Determination. Crystal, data collection, and refinement parameters are given in Table 3. Suitable crystals for single-crystal X-ray diffraction were selected and mounted either in a nitrogen-flushed, thin-walled capillary or on the tip of a fine glass fiber with epoxy cement. The data were collected on a Siemens P4 diffractometer equipped with a SMART/CCD detector.

The systematic absences in the diffraction data are uniquely consistent with the reported space group for **4**, and no evidence of symmetry higher than triclinic was observed in the diffraction data of **3**. E-statistics suggested the centrosymmetric space group option, $P\bar{1}$, which yielded chemically reasonable and computationally stable results of refinement. The structures were solved by direct methods, completed by subsequent difference Fourier syntheses, and refined by full-matrix least-squares procedures. An empirical absorption correction was applied to the data of **3**, based on a Fourier series in the polar angles of the incident and diffracted beam paths, and was used to model an absorption surface for the difference between the observed and calculated structure factors.[28] No other absorption corrections were required because there was less than 10% variation in the integrated ψ-scan intensities. One-half of a molecule of dichloromethane, disordered over an inversion center, was located in the asymmetric unit of **3**. All other nonhydrogen atoms were refined with anisotropic displacement parameters. All other hydrogen atoms were treated as idealized contributions.

All software and sources of the scattering factors are contained in the SHELXTL (5.03 and 5.10) program libraries (G. Sheldrick, Siemens XRD, Madison, WI).

Acknowledgment. We thank the NSF Career Program, the Petroleum Research Fund, administered by the American Chemical Society, the Exxon Education Foundation, DuPont, and Union Carbide (Innovation Recognition Program) for partial support. We are grateful to Profs. R. P. Hughes, M. Brookhart, and M. Gagne for helpful discussions. The University of Delaware thanks the NSF (CHE-9628768) for their support of the purchase of the CCD-based diffractometer.

Supporting Information Available: Details of the crystal structure determinations. This material is available free of charge via the Internet at http://pubs.acs.org.

OM9903691

(28) Walker, N.; Stuart, D. *Acta Crystallogr.* **1983**, *A39*, 158−166.